

**INTER-AMERICAN TROPICAL TUNA COMMISSION**  
**AD-HOC PERMANENT WORKING GROUP ON FADS**

**FIFTH MEETING**

*(by videoconference)*

06-07 May 2021

**DOCUMENT FAD-05-INF-E**

**TROPICAL TUNA BIOMASS INDICATORS FROM ECHOSOUNDER BUOYS IN THE  
EASTERN PACIFIC OCEAN**

*Jon Uranga<sup>1</sup>, Jon Lopez<sup>2</sup>, Maitane Grande<sup>1</sup>, Cleridy E. Lennert-Cody<sup>2</sup>, Iñaki Quincoces<sup>1</sup>, Igor Granada<sup>1</sup>, Mark N. Maunder<sup>2</sup>, Alexandre Aires-da-Silva<sup>2</sup>, Gorka Merino<sup>1</sup>, Hilario Murua<sup>3</sup> Josu Santiago<sup>1</sup>*

**SUMMARY**

*The collaboration with the vessel-owners associations and the buoy-providers companies operating in the Pacific Ocean, has made it possible to obtain information recorded by the satellite linked GPS tracking echosounder buoys used by some of the tropical tuna purse seiners in the Eastern Pacific Ocean since 2010. These instrumental buoys inform fishers remotely in real-time about the accurate geolocation of the FAD and the presence and abundance of fish aggregations underneath them. Echosounder buoys have the potential of being a good observation platform to evaluate abundances of tunas and accompanying species using catch-independent data. Current echosounder buoys provide a single acoustic value without discriminating species or size composition of the fish underneath the FAD. Therefore, it has been necessary to combine the echosounder buoy data with fishery data, species composition and average size, to obtain a specific indicator. This paper presents a novel index of abundance of skipjack tuna in the Eastern Pacific Ocean derived from echosounder buoys for the period 2012-2020.*

**1. INTRODUCTION**

Historically, stock assessments for tropical tuna species have relied almost exclusively on indirect abundance estimators, dependent on commercial catches and fishing effort derived from captain's logbooks or observer data (Maunder and Punt 2004). These catch and effort data are used to provide information on relative trends in fish abundance that are integrated in fish stock assessment models to assess the state and the evolution of fish stocks (Quinn and Deriso 1999). Relative abundance indices based on Catch-Per-Unit-Effort (CPUE) are related with the abundance, through the catchability coefficient ( $q$ ). However, this proportionality is affected by various factors as variations in fishing efficiency, spatial dynamics of the fleet or species, and changes in target species (Maunder and Punt 2004; Maunder et al. 2006). To try to remove the effects of these factors on the CPUE data so that changes related to population abundance can be identified, standardization of CPUE is used.

In the case of the tropical tuna purse-seine fishery, fishing efficiency has increased with the

---

<sup>1</sup>AZTI, Marine Research, Basque Research and Technology Alliance (BRTA). Txatxarramendi ugarteia z/g, 48395. Sukarrieta - Bizkaia, Spain

<sup>2</sup> Inter-American Tropical Tuna Commission, 8901 La Jolla Shores Drive, La Jolla CA 92037, USA

<sup>3</sup> International Seafood Sustainability Foundation (ISSF). 1440 G Street NW Washington DC 20005. U.S. hmurua@issf-foundation.org

incorporation of new technology on board and with the use of Fish Aggregating Devices (FADs) (Lopez et al. 2014; Torres-Irineo et al. 2014; Gaertner et al. 2016). The difficulties of providing new covariates based on fine scale data to reflect these technological changes and effort creep and the lack of a good proxy for purse seine effort on FADs, have hampered to standardize the FAD fishing CPUEs (Gaertner et al. 2016; Katara 2018; Wain 2021). This has prevented the use of the purse-seine FAD CPUE in stock assessment models and resulted in a lack of skipjack and juvenile yellowfin and bigeye tuna abundance indices. Science-industry collaborative projects are making possible to gain knowledge about the adoption of technological advances in this fleet and to improve the CPUE standardization (Wain 2021) so as to improve tropical tuna assessments.

The introduction of FADs in the purse-seine fishery and the satellite-linked echosounder buoys attached to those FADs (Scott 2014) provides an alternative method for estimation of indices that are catch-independent. These instrumental buoys give daily information on buoy position and the potential size of fish aggregation underneath the FADs, being unique observation platforms of tuna and other aggregated species. In recent years research actions have been conducted to recover buoy-derived information, develop of methodological frameworks to extract reliable scientific information from buoys, describe tuna behaviour around FADs and provide buoy-derived abundance indices (Lopez et al. 2014; Capello et al. 2016; Moreno 2016; Orúe Montaner 2019; Santiago et al. 2019; Baidai 2020).

The Buoy-derived Abundance Index (BAI), which is based on the proportional relationship between the FAD associated echosounder buoy biomass and the total abundance of tuna, has been recently incorporated in several tropical tuna stock assessments (ICCAT 2020). Building on that success, a framework of collaborative work was established with the support of the International Seafood Sustainability Foundation (ISSF) between the Inter-American Tropical Tuna Commission (IATTC) and AZTI, together with echosounder buoy providers and tropical tuna purse seiner fishing companies operating in the eastern Pacific Ocean (EPO) (companies integrated in OPAGAC and Cape Fisheries), to work on the BAI of tropical tuna species in the region. The preliminary results presented in this paper correspond to a novel index of abundance of skipjack tuna in the eastern Pacific Ocean derived from echosounder buoys for the period 2012-2020, which can form the basis for future abundance indices for the main tropical tuna species in the eastern Pacific Ocean.

## **2. MATERIAL AND METHODS**

### ***2.1 Acoustic data pre-filtering***

The data used in this analysis is recorded by satellite linked echo-sounder buoys, which are deployed with FADs in the tropical tuna purse-seine fishery. Data for this analysis have been provided by the buoy manufacturer Satlink. The buoy technical specifications, per model, are shown in Table 1. All buoys register data from 3 to 115 m depth divided into 10 homogeneous vertical layers, each with a resolution of 11.2 m (the first 3 m correspond to the blind zone). During the period analysed, five different buoy models have been used by the fleet: DS+, DSL, ISD, ISL and SLX ([Table 1](#)).

The fishing companies that have provided acoustic information from their echosounder buoys were: Albacora, Calvo, Garavilla, Ugavi, and Cape Fisheries. This adds up to a total of 23 purse-seine vessels from 5 different flags (Panama, Spain, Ecuador, El Salvador, USA) operating in the IATTC convention area.

A total number of 8.31 million acoustic records from 31,116 individual buoys for the period from January 2012 to December 2020 were used to build the database of acoustic information for the EPO. Years 2010 and 2011 were discarded due to the low number of records available ([Figure 1](#)) and acoustic records from areas with low number of observations (less than 200 records in 5°x5° statistical rectangles) and west of 150°W were excluded for this analysis.

From each single data record transmitted via satellite, the following information can be extracted: “Name”, unique identification number of the buoy, given by the model code (DS+, DSL, ISL, ISD, SLX) followed by 5-6 digits; “OwnerName”, name of the buoy owner assigned to a unique purse seine vessel; “MD”, message descriptor (160, 161 and 162 for position data, without sounder data, and 163, 168, 169 and 174 for sounder data); “StoredTime”, date (dd/mm/yyyy) and hour (HH:MM) of the echosounder record; “Latitude, Longitude”, GPS latitude and longitude of recorded data during each day (in decimals); “Bat”, charge level as a percentage (not provided, except for the D+ and DS+ models, in voltage); “Temp”, temperature (Not provided); “Speed”, speed in knots; “Drift”, bearing in degrees (Not provided); “Layer1-Layer10”, estimated tons by layers (values are estimated by a manufacturer’s method which converts raw acoustic backscatter into biomass in tons, using a depth layer echo-integration procedure based exclusively on an algorithm based on the target strength (TS) and weight of skipjack tuna; “Sum”, sum of the biomass estimated at each layer; “Max”, maximum biomass estimated at any layer; and “Mag1, Mag3, Mag5 and Mag7”, magnitudes corresponding to the counts of detected targets according to the TS of the detection peak.

A set of five filters were applied to the original data to remove artifacts: isolated, duplicated and ubiquitous rows, that are mainly caused by satellite communication incidents; buoys located 1 km or closer to land or located in areas with a bottom depth shallower than 200 m, detected and removed using shoreline data from the GSHHG database (Wessel 1996) and a worldwide global bathymetry information (Amante and Eakins 2009); and “on-board” or “at sea” positions, identified using a Random Forest algorithm (Orue et al. 2019; Santiago et al. 2020), these cases are mainly related to buoy activation incidents on-board vessels prior and post deployment.

In addition to the previously mentioned cleaning filters, the following selection criteria (Santiago et al. 2020) were used to build the final dataset to feed into the standardization analysis: i) shallower layers (<25m) were excluded because they are consider to potentially reflect non-tuna species (Orue et al. 2019); ii) only data recorded around sunrise, between 4 a.m. and 8 a.m. in local time, were considered for the analysis because they are supposed to capture the echosounder biomass signals that better represents the abundance of fish under the FADs (Moreno et al. 2007); and finally, iii) acoustic data belonging to what we defined as “virgin segments” were selected in order to use the segment of a buoy trajectory whose associated FAD likely represents a new deployment which has been potentially colonized by tuna and not fished yet. To calculate virgin segments, single buoy segments were divided into smaller sub-segments where the difference between two consecutive observations of the same buoy was larger than 30 days. Then, the newly renamed sub-segments with less than 30 observations and those having a time difference between any of the consecutive observations longer than 4 days during the first 35 days were removed. Finally, from the remaining data we consider as virgin segments those segments of trajectories from 20-35 days at sea (Orue et al. 2019). [Figure 2](#) shows a diagram with an example of “virgin” segments used for the calculation of the BAI index.

## **2.2 From acoustic data to a species-specific abundance indicator**

To calculate the biomass aggregated under a FAD from the acoustic signal, Satlink uses the density of one species, skipjack, to provide the biomass in tons, and thus, biomass data from Satlink has to be converted to decibels reversing their formula for the biomass computation. Then we recomputed biomass using standard acoustic abundance estimation equations (Simmons and MacLennan 2005):

$$Biomass_i = \frac{s_v \cdot Vol \cdot p_i}{\sum_i \sigma_i \cdot p_i}$$

where  $s_v$  is the volume backscattering strength,  $Vol$  is the sampled volume of the beam and  $p_i$  and  $\sigma_i$  are the proportion and linearized target strength of each species  $i$  respectively. Species proportions in weight at 1°x1° and month resolution were extracted from logbooks (for class 1-5 vessels, ≤ 363 mt)

and observers data (for class 6 vessels, >363mt) of IATTC from 14 different flags. Mean fish lengths ( $L_i$ ), by 5°x5° area - month resolution, for skipjack (SKJ), bigeye (BET) and yellowfin (YFT) were obtained from IATTC port-sampling data that were first raised to the catch in the sampled wells. Weights were estimated using weight-length relationships (IATTC conversion factors). Then, the following Target Strength-length relationships were used to obtain linearized TS per kilogram:

$$\sigma_i = \frac{10^{(TS)/10}}{w_i}$$

where  $w_i$  is the mean weight of each species and TS is the backscattering cross-section of each species individual fish. It is assumed that the linear value of TS, is proportional to the square of fish length (Simmons and MacLennan 2005).

$$TS = 20\log(L_i) + b_{20}$$

Given that each brand uses different operating frequencies, we used different  $b_{20}$  values for each species. For Satlink, the  $b_{20}$  values were obtained from Boyra et al. (2018) for SKJ, from Bertrand and Josse (2000) and Oshima (2008) for YFT and from Boyra et al. (2018) for BET.

Since acoustic records do not always have information on catch composition for the same time-area strata, we followed a three-step hierarchical process to get this correspondence: 1) use species distribution data from the same 5°x5° grid, year and month; 2) alternatively, use the same quarter and 5°x5° grid; and finally, as a last resort 3), use the mean values of species distribution data at same quarter and region shown in [Figure 3](#).

The results presented in this document correspond to the fraction of the acoustic signal estimated to be informative for the biomass of skipjack.

### **2.3 The BAI index: Buoy-derived Abundance Index**

The estimator of abundance BAI was defined as the 0.9 quantile of the integrated acoustic energy observations in each of the "virgin" sequences. A high quantile was chosen because the large values are likely produced by tuna (opposite of what is expected for other species). This assumption is made by all the buoy brands in the market, which use the maximum value as the summary of each time interval. In our case we selected a high quantile instead of the maximum to try to provide a more robust estimator by avoiding outlier values. We also did this to avoid low values that might appear after eventual hauls occurring along the sequence. The total number of "virgin" sequences analysed, and hence the number of observations in the model, rose to 11732, of which 11696 (99.69%) were positives.

### **2.4 The model**

The covariates used in the standardization process and fitted as categorical variables were year-quarter, 5x5° area and buoy model. A proxy of 1°x1° and monthly FAD densities (average number of unique buoys over each month) and the following environmental variables were fitted as continuous variables:

- Ocean mixed layer thickness: defined as the thickness of the thermocline in the point of density increase, compared to density at 10 m depth, corresponds to a temperature decrease of 0.2°C in local surface conditions ( $\theta_{10m}$ ,  $S_{10m}$ ,  $P_0 = 0$  db, surface pressure).
- Chlorophyll: Mass concentration of chlorophyll a in sea water at sea surface.

- Sea Surface Temperature (SST)
- SST and Chlorophyll fronts: Oceanographic front detection was performed using the “*grec*” package for R (Team 2013) for each daily dataset, that provides algorithms for detection of spatial patterns from oceanographic data using image processing methods based on Gradient Recognition (Belkin and O'Reilly 2009).

The model we propose is based on an assumption very similar to the fundamental relationship among CPUE and abundance widely used in quantitative fisheries analysis. In our case we built the index based on the assumption that the signal from the echosounder is proportional to the abundance of fish.

$$BAI_t = \varphi \cdot B_t$$

where  $BAI_t$  is the Buoy-derived Abundance Index and  $B_t$  is the abundance in time  $t$  (Santiago et al., 2016).

Although it would appear to be obvious, there is not a lot of literature on the relationship between acoustic indicators and fishing performance. It is assumed that acoustic echo integration is a linear process, i.e., proportional to the number of targets (Simmons and MacLennan 2005) and has been experimentally proven to be correct with some limitations (Foote, 1983; Røttingen, 1976). Therefore, acoustic data (echo-integration) are commonly taken as a proxy for abundance and are used to obtain acoustic estimates of abundance of many pelagic species (Hampton 1996; ICES 2015; Masse et al. 2018).

As with the catchability, the coefficient of proportionality  $\phi$  is not constant for many reasons. In order to ensure that  $\phi$  can be assumed to be constant (i.e. to control the effects other than those caused by changes in the abundance of the population) a standardization analysis should be performed by aiming to remove factors other than changes in abundance of the population. This can be performed standardizing nominal measurements of the echosounders using a Generalized Linear Mixed Modelling (GLMM) approach.

Considering the low proportion of zero values (0.31%), the delta lognormal approach (Lo et al. 1992) was not considered. GLMM (log-normal error structured model) was applied to standardize the acoustic observations. A stepwise procedure was used to fit the model with all the explanatory variables and interactions in order to determine those that significantly contributed to explaining the variability in the data. For this, deviance analysis tables were created for the positive acoustic records. Final selection of explanatory variables was conducted using: a) the relative percent increase in deviance explained when the variable was included in the model (normally variables that explained more than 5% were selected), and b) The Chi-square ( $\chi^2$ ) significance test. Those variables that explained less than 5% of the variability in the data were not considered for the final model.

Interactions between the temporal component (year-quarter) with the rest of the variables were also evaluated. If an interaction was statically significant, it was then considered as a random interaction(s) within the final model (Maunder and Punt 2004).

Lastly, the selection of the final mixed model was based on the Akaike's Information Criterion (AIC), the Bayesian Information Criterion (BIC), and a Chi-square ( $\chi^2$ ) test of the difference between the log-likelihood statistic of different model formulations. The year-quarter effect least square means (LSmeans) were bias corrected for the logarithm transformation algorithms using Lo et al (Lo et al. 1992). All analyses were done using the lme4 package of R (Bates et al. 2014).

### 3. RESULTS

A total of 8.31 million acoustic records from 31116 buoys for the period from January 2012 to December 2020 were evaluated to create 11696 observations for the GLMM analysis. Each observation was calculated as the 90% percentile of a “virgin” segment of buoy trajectories. A virgin segment was defined as the segment of a buoy trajectory from 20-35 days at sea, so that the associated FAD likely represents a new deployment which has been potentially colonized by tuna and not already fished.

In this analysis we have obtained from the acoustic signal of the echosounder buoys associated to FADs the fraction of the biomass that would correspond to skipjack tuna aggregated under a FAD.

[Figure 4](#) shows the histograms of the BAI and log transformed BAI nominal values. Log transformation makes the data to follow a normal distribution, as shown in the left panel of [Figure 4](#). [Figure 5](#) shows the spatial distribution [5°x5°] of the number of “virgin” sequences of buoy trajectories that have been used in the GLMM analysis. The quarterly evolution of the number of observations on a 5°x5° grid is shown in figure 6. The period 2013-2017 is when the largest number of observations is available.

[Figure 7](#) shows the quarterly evolution of the nominal log BAI index by squares of 5x5 degrees from 2012 to 2020.

The results of the deviance analysis are shown in [Table 2](#). The model explained 37% of the total deviance. The most significant explanatory variables were: year-quarter, 5°x5° area and the interaction year-quarter\*area that was considered as random effect. No significant residual patterns were observed ([Figure 8](#)).

Quarterly series of standardized BAI index are provided in [Table 2](#) and [Figure 9](#). There are three periods with higher values: a) at the beginning of the series, 2012, with wide confidence intervals due to the relatively low number of observations; b) in the years 2015 and 2016; and c) in 2019. Apart from the first quarter from 2012 the CVs remain relatively stable (between 13-16%) during the whole time series.

### 4. FUTURE STEPS

This paper presents preliminary results on abundance indicators from the acoustic signal of buoys following the methodology previously developed for tropical tuna stocks in other oceans (Santiago et al. 2019; Santiago et al. 2020a; Santiago et al. 2020b). This methodology is intended to be improved in the context of the IATTC-AZTI collaboration and the following aspects have already been identified as potential lines of investigation:

- Improve determination of virgin segments (a): the current threshold of 30 days between two consecutive observations of the same buoy to consider trajectories of two different FADs is too restrictive. A high threshold increases the certainty of differentiating new trajectories but severely limits the number of observations available for analysis. On the other hand, a threshold of a few days decreases the reliability of separating different trajectories, increasing the number of observations. A first exploratory analysis with 10.000 random buoys show an increase of 25% on the number of virgin segments when using a threshold of 1 week instead of 1 month. It is planned to evaluate the effect of using different thresholds for virgin segment selection on the robustness of results.
- It is also planned to use observer data on FAD deployments to investigate whether methodology of classification of virgin segments is accurate. Observer data can be used to inform the virgin segment selection and the selection of the threshold of days between two consecutive observation of the same buoy.

- Improve determination of virgin segments (b): a “virgin” segment is defined as segment of a buoy trajectory whose associated FAD likely represents a new deployment or re-deployment which has been potentially colonized by tuna and probably not fished yet. Currently the period selected corresponds to 20-35 days since the estimated date of deployment of the FAD. According to Orue et al. (2019) in the Indian Ocean, tuna seem to arrive at FADs in  $13.5 \pm 8.4$  days, so we leave a period of 20 days since deployment to try to maximize the probability of the FAD being colonized. The period of observation was also limited to 35 days since the deployment to minimize the probability of having been fished. Different time periods will be explored after analyzing the spatial-temporal pattern of FAD colonization in the EPO. Colonization models for each area will be produced, exploring a number of techniques, from traditional GAMMs and GLMMs to most sophisticated Boosted Regression. With regard to the methodology for acoustic based biomass estimation, sensitivity tests will be performed to test the appropriateness of using normal and non-normal distributions. Also new biomass estimates will be explored using other metrics rather than the 90% percentile (mean, median, etc.).
- Explore the best spatial/temporal strata in the EPO to characterize the species composition and sizes to be applied for the species-specific acoustic biomass estimations because those are the two fishery dependent sets of data to convert acoustic information into biomass. The three steps approach currently used with different time-area strata resolution will be reviewed and sensitivity analysis with catch data performed to test the robustness of the estimation to different assumptions.
- Develop methodology to predict species catches from acoustic samples using machine learning algorithms. Using observer data on catch composition for individual sets, it may be possible to relate particular echograms with specific species composition so that we can move away from spatio-temporal fishery statistics.

These issues reflected above are only examples of the improvement tasks that are being undertaken in the context of this collaborative Joint Project between AZTI e IATTC with the collaboration of the fleet, buoy providers and the ISSF. In this sense, the involvement of the industry is fundamental to provide these valuable indicators. We deeply appreciate the involvement of OPAGAC and Cape Fisheries in this project and hope that other companies will join this initiative, retrieving historical information and regularly providing high-resolution buoy data, including acoustic information. These advancements can provide significant information to complement current stock assessments of tropical tuna stocks, providing indices less dependent on fisheries data and less affected by changes in fishing efficiency.

### **Acknowledgements**

We want to express our gratitude to the following fishing companies that have provided acoustic information from their echosounder buoys: Albacora, Calvo, Garavilla, Ugavi and Cape Fisheries. And to ISSF for partially funding this work.

### **References**

- Amante, C. and B. Eakins (2009). "ETOPO1 1 arc-minute global relief model: procedures, data sources and analysis. NOAA Technical Memorandum NESDIS NGDC-24." National Geophysical Data Center, NOAA 10: V5C8276M.
- Baidai, Y. D. A. (2020). Derivation of a direct abundance index for tropical tunas based on their associative behavior with floating objects, Université Montpellier.
- Bates, D., M. Mächler, et al. (2014). "Fitting linear mixed-effects models using lme4." arXiv preprint arXiv:1406.5823.

- Belkin, I. M. and J. E. O'Reilly (2009). "An algorithm for oceanic front detection in chlorophyll and SST satellite imagery." *Journal of Marine Systems* **78**(3): 319-326.
- Bertrand, A. and E. Josse (2000). "Tuna target-strength related to fish length and swimbladder volume." *ICES Journal of Marine Science* **57**(4): 1143-1146.
- Boyra, G., G. Moreno, et al. (2018). "Target strength of skipjack tuna (*Katsuwonus pelamis*) associated with fish aggregating devices (FADs)." *ICES Journal of Marine Science* **75**(5): 1790-1802.
- Capello, M., J. L. Deneubourg, et al. (2016). "Population assessment of tropical tuna based on their associative behavior around floating objects." *Scientific Reports* **6**(1): 36415.
- Gaertner, D., J. Ariz, et al. (2016). "Objectives and first results of the CECOFAD project." *Collective Volume of Scientific Papers* **72**(2): 391-405.
- Gaertner, D., S. Clermidy, et al. (2016). "Results achieved within the framework of the EU research project: Catch, Effort, and eCOsystem impacts of FAD-fishing (CECOFAD)." *Acta Agriculturae Slovenica*.
- Hampton, I. (1996). "Acoustic and egg-production estimates of South African anchovy biomass over a decade: comparisons, accuracy, and utility." *ICES Journal of Marine Science* **53**(2): 493-500.
- ICCAT (2020). *Report of the 2019 ICCAT yellowfin tuna stock assessment meeting.*, (Grand-Bassam, Cote d'Ivoire, 8-16 July 2019).
- ICES (2015). Manual for International Pelagic Surveys (IPS). Series of ICES Survey Protocols. **SISP 9 - IPS. 92 pp.**
- Katara, I., Gaertner, D., Marsac, F., Grande, M., Kaplan, D., Urtizberea, A., Abascal, F. (2018). Standardisation of yellowfin tuna CPUE for the EU purse seine fleet operating in the Indian Ocean. 20th session of the Working Party on Tropical Tuna.
- Lo, N. C.-h., L. D. Jacobson, et al. (1992). "Indices of relative abundance from fish spotter data based on delta-lognormal models." *Canadian journal of fisheries and aquatic sciences* **49**(12): 2515-2526.
- Lopez, J., G. Moreno, et al. (2014). "Evolution and current state of the technology of echo-sounder buoys used by Spanish tropical tuna purse seiners in the Atlantic, Indian and Pacific Oceans." *Fisheries Research* **155**: 127-137.
- Masse, J., A. Uriarte, et al. (2018). "Pelagic survey series for sardine and anchovy in ICES subareas 8 and 9—Towards an ecosystem approach." *ICES cooperative research report*(332).
- Maunder, M. N. and A. E. Punt (2004). "Standardizing catch and effort data: a review of recent approaches." *Fisheries Research* **70**(2-3): 141-159.
- Maunder, M. N., J. R. Sibert, et al. (2006). "Interpreting catch per unit effort data to assess the status of individual stocks and communities." *ICES Journal of Marine Science* **63**(8): 1373-1385.
- Moreno, G., L. Dagorn, et al. (2007). "Fish behaviour from fishers' knowledge: the case study of tropical tuna around drifting fish aggregating devices (DFADs)." *Canadian journal of fisheries and aquatic sciences* **64**(11): 1517-1528.
- Moreno, G., Dagorn, L., Capello, M., Lopez, J., Filmalter, J., Forget, F., Sancristobal, I., . and Holland, K. (2016). "Fish aggregating devices (FADs) as scientific platforms." *Fisheries Research* **178**: **122-129**.
- Orue, B., J. Lopez, et al. (2019). "From fisheries to scientific data: A protocol to process information from fishers' echo-sounder buoys." *Fisheries Research* **215**: 38-43.
- Orue, B., J. Lopez, et al. (2019). "Aggregation process of drifting fish aggregating devices (DFADs) in the Western Indian Ocean: Who arrives first, tuna or non-tuna species?" *PloS one* **14**(1): e0210435.
- Orúe Montaner, B. (2019). "Ecology and behavior of tuna and non-tuna species at drifting fish aggregating devices (DFADs) in the Indian Ocean using fishers' echo-sounder buoys."
- Oshima, T. (2008). "Target strength of Bigeye, Yellowfin and Skipjack measured by split beam echo sounder in a cage." *IOTC, WPTT-22* **4**.
- Quinn, T. J. and R. B. Deriso (1999). *Quantitative fish dynamics*, oxford university Press.
- Santiago, J., J. Uranga, et al. (2020a). A NOVEL INDEX OF ABUNDANCE OF SKIPJACK IN THE INDIAN OCEAN DERIVED FROM ECHOSOUNDER BUOYS, IOTC-2020-WPTT22(DP)-14.



- Santiago, J., J. Uranga, et al. (2019). A Novel Index of Abundance of Juvenile Yellowfin Tuna in the Indian Ocean Derived from Echosounder Buoys, IOTC–2019–WPTT21–47.
- Santiago, J., J. Uranga, et al. (2020). "A novel index of abundance of juvenile yellowfin tuna in the Atlantic Ocean derived from echosounder buoys." Collect. Vol. Sci. Pap. ICCAT **76(6)**: 321-343.
- Santiago, J., J. Uranga, et al. (2020b). "A novel index of abundance of juvenile yellowfin tuna in the Atlantic Ocean derived from echosounder buoys." Collect. Vol. Sci. Pap. ICCAT **76(6)**: 321-343.
- Scott, G. P., & Lopez, J. (2014). The use of FADs in Tuna Fisheries. European Parliament. Policy Department B: Structural and Cohesion Policies: Fisheries. **IP/B/PECH/IC/2013**.
- Simmons, E. and D. MacLennan (2005). "Fisheries acoustics." Theory and Practice. Second edition published by Blackwell Science.
- Team, R. C. (2013). R: A language and environment for statistical computing.
- Torres-Irineo, E., D. Gaertner, et al. (2014). "Changes in fishing power and fishing strategies driven by new technologies: The case of tropical tuna purse seiners in the eastern Atlantic Ocean." Fisheries Research **155**: 10-19.
- Wain, G., Guéry, L., Kaplan, D. M., & Gaertner, D. (2021). "Quantifying the increase in fishing efficiency due to the use of drifting FADs equipped with echosounders in tropical tuna purse seine fisheries." ICES Journal of Marine Science **78(1)**, **235-245**.
- Wessel, P., and W. H. F. Smith (1996). "A global, self-consistent, hierarchical, high-resolution shoreline database." J. Geophys. Res **101(B4)**, **8741-8743**.

**Table 1.** Technical specifications of different buoy models and observed values over analysis data.

| Model | Typical setup |                                  |       |  |                                    |                           | Mean observed values over analysis data |                    |
|-------|---------------|----------------------------------|-------|--|------------------------------------|---------------------------|---|--------------------|
|       | Beam angle    | Sounder frequency                | Power | Frequency of acoustic sampling (ping rate) | Daily acoustic data recorded       | Frequency of transmission | Number of buoys                         | Sampling frequency |
| DS+   | 32°           | 190.5 kHz                        | 100 W | 3  | 3                                  | 24h                       | 1428                                    | 1.36               |
| DSL+  | 32°           | 190.5 kHz                        | 100 W | 3  | 3                                  | 24h                       | 12462                                   | 2.82               |
| ISL+  | 32°           | 190.5 kHz                        | 100 W | 15 min                                     | variable (reset at dusk)           | 24h                       | 23                                      | 1.67               |
| ISD+  | 32°           | 200/38 kHz (38 kHz not provided) | 100 W | 15 min                                     | variable (reset at dusk)           | 24h                       | 6214                                    | 1.21               |
| SLX+  | 32°           | 200                              | 100 W | 5 min                                      | variable (Sunrise or Alarms based) | 24h                       | 785                                     | 1.98               |

**Table 2.** Deviance table for the GLM lognormal model of the 2012-2020 period

| Variable   | Df  | Deviance | Resid..Df | Resid..Dev | F  | Pr..F. | Dev..Exp |
|------------|-----|----------|-----------|------------|----|--------|----------|
| NULL       | NA  | NA       | 11300     | 15847      | NA | NA     | NA       |
| yyqq       | 35  | 1019     | 11265     | 14828      | 30 | 0.0000 | 6.43 %   |
| area       | 27  | 2170     | 11238     | 12658      | 82 | 0.0000 | 13.69 %  |
| model      | 2   | 73       | 11236     | 12585      | 37 | 0.0000 | 0.46 %   |
| den        | 1   | 78       | 11235     | 12507      | 80 | 0.0000 | 0.49 %   |
| sst        | 1   | 0        | 11234     | 12507      | 0  | 0.5915 | 0 %      |
| sstfront   | 1   | 2        | 11233     | 12505      | 2  | 0.1696 | 0.01 %   |
| mld        | 1   | 1        | 11232     | 12504      | 1  | 0.2495 | 0.01 %   |
| yyqq:area  | 867 | 2179     | 10365     | 10324      | 3  | 0.0000 | 13.75 %  |
| yyqq:model | 29  | 86       | 10336     | 10238      | 3  | 0.0000 | 0.54 %   |
| yyqq:den   | 34  | 98       | 10302     | 10141      | 3  | 0.0000 | 0.62 %   |
| yyqq:sst   | 35  | 98       | 10267     | 10042      | 3  | 0.0000 | 0.62 %   |
| yyqq:mld   | 34  | 73       | 10233     | 9970       | 2  | 0.0001 | 0.46 %   |

**Table 3.** Nominal and standardized Buoy-derived Abundance Index for the period 2012-2020. Standard errors and coefficient of variations of the standardized series are also included.

| Quarter | Index nominal | BAI Index | BAI se | BAI cv |
|---------|---------------|-----------|--------|--------|
| 12Q1    | 1.686         | 2.912     | 1.380  | 0.474  |
| 12Q2    | 4.973         | 3.594     | 0.600  | 0.167  |
| 12Q3    | 3.895         | 3.066     | 0.487  | 0.159  |
| 12Q4    | 2.019         | 1.330     | 0.214  | 0.161  |
| 13Q1    | 2.171         | 1.517     | 0.234  | 0.155  |
| 13Q2    | 1.880         | 1.368     | 0.196  | 0.144  |
| 13Q3    | 0.856         | 0.701     | 0.109  | 0.155  |
| 13Q4    | 1.505         | 1.068     | 0.166  | 0.155  |
| 14Q1    | 1.202         | 0.898     | 0.138  | 0.153  |
| 14Q2    | 1.486         | 1.231     | 0.194  | 0.158  |
| 14Q3    | 1.101         | 0.852     | 0.135  | 0.158  |
| 14Q4    | 1.387         | 1.111     | 0.173  | 0.156  |
| 15Q1    | 2.612         | 1.748     | 0.267  | 0.153  |
| 15Q2    | 2.958         | 2.007     | 0.300  | 0.149  |
| 15Q3    | 2.054         | 2.072     | 0.276  | 0.133  |
| 15Q4    | 1.896         | 1.781     | 0.255  | 0.143  |
| 16Q1    | 2.067         | 1.685     | 0.249  | 0.148  |
| 16Q2    | 1.629         | 1.532     | 0.236  | 0.154  |
| 16Q3    | 1.908         | 1.665     | 0.263  | 0.158  |
| 16Q4    | 1.806         | 1.440     | 0.228  | 0.159  |
| 17Q1    | 1.323         | 0.911     | 0.135  | 0.148  |
| 17Q2    | 1.493         | 1.143     | 0.164  | 0.144  |
| 17Q3    | 1.895         | 1.336     | 0.200  | 0.149  |
| 17Q4    | 1.459         | 1.171     | 0.177  | 0.151  |
| 18Q1    | 1.356         | 0.930     | 0.134  | 0.144  |
| 18Q2    | 1.350         | 1.049     | 0.153  | 0.146  |
| 18Q3    | 1.384         | 1.052     | 0.158  | 0.151  |
| 18Q4    | 1.806         | 1.385     | 0.215  | 0.155  |
| 19Q1    | 1.589         | 1.136     | 0.175  | 0.154  |
| 19Q2    | 2.748         | 1.786     | 0.279  | 0.156  |
| 19Q3    | 1.614         | 1.370     | 0.221  | 0.161  |
| 19Q4    | 2.331         | 1.999     | 0.308  | 0.154  |
| 20Q1    | 2.909         | 1.960     | 0.268  | 0.137  |
| 20Q2    | 2.557         | 1.796     | 0.275  | 0.153  |
| 20Q3    | 1.881         | 1.327     | 0.191  | 0.144  |
| 20Q4    | 1.678         | 1.145     | 0.177  | 0.154  |

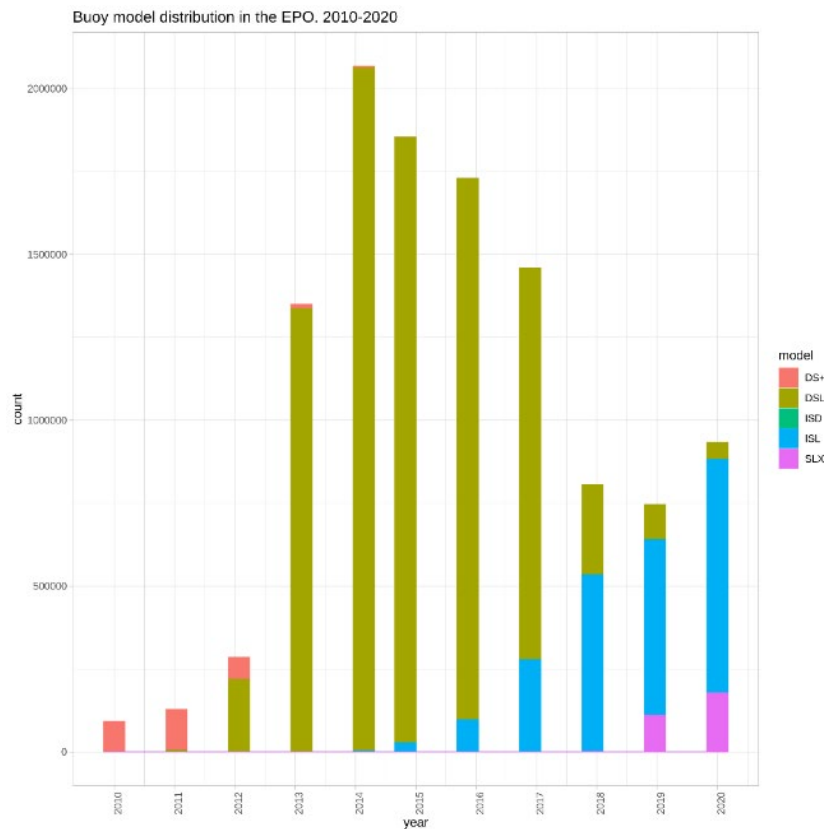


**Figure 1.** Buoy data distribution per model in the Pacific Ocean (2010-2020)

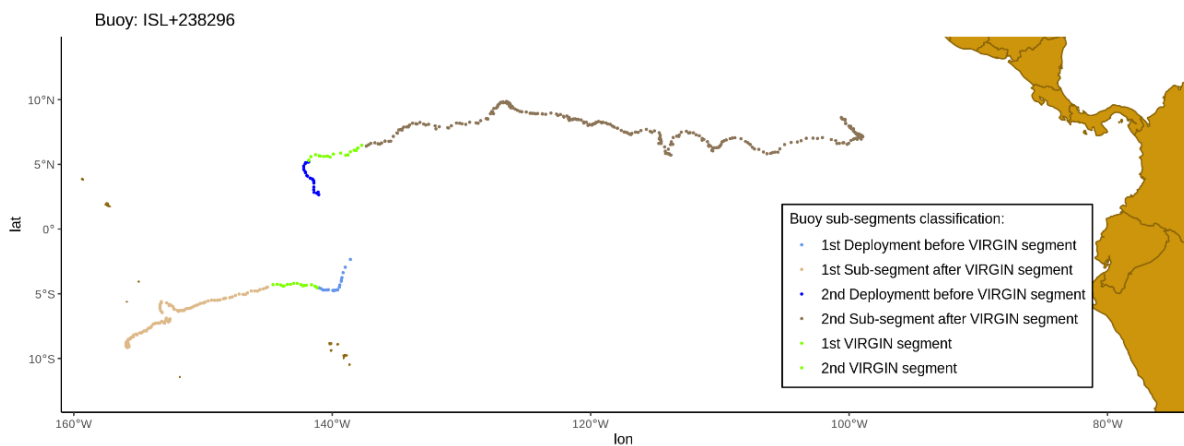


**Figure 2.** Example of “virgin” segments used for the calculation of the BAI index. Trajectories correspond to buoy ISL+284966 with two different paths representing drifts of different FADs. A virgin segment is defined as the segment of a buoy trajectory whose associated FAD likely represents a new deployment, which has been potentially colonized by tuna and not already fished. We consider as virgin segments (i.e. when tuna has aggregated to FAD) those segments of trajectories from 20-35 days at sea. “Virgin” segments are shown in green.

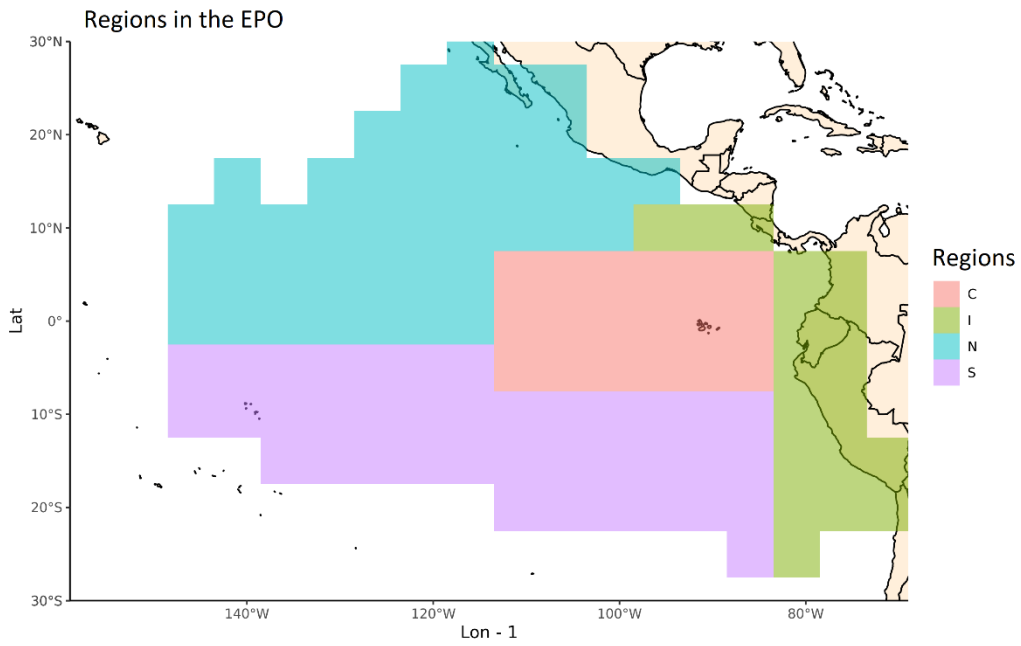


**Figure 3.** Length-frequency sampling areas defined by the IATTC staff for analyses of tropical tuna catches associated with floating objects.

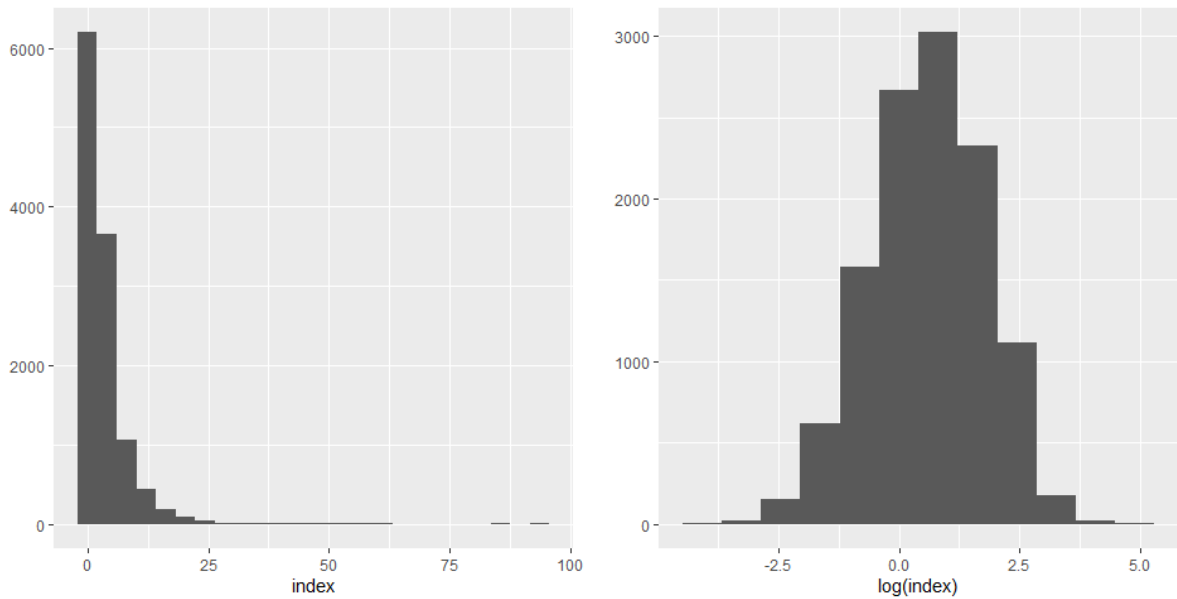


**Figure 4.** Histograms of the nominal values (left) and the log transformed nominal values (right) of the Buoy-derived Abundance Index (0.9 quantile of the integrated acoustic energy observations in "virgin" sequences).

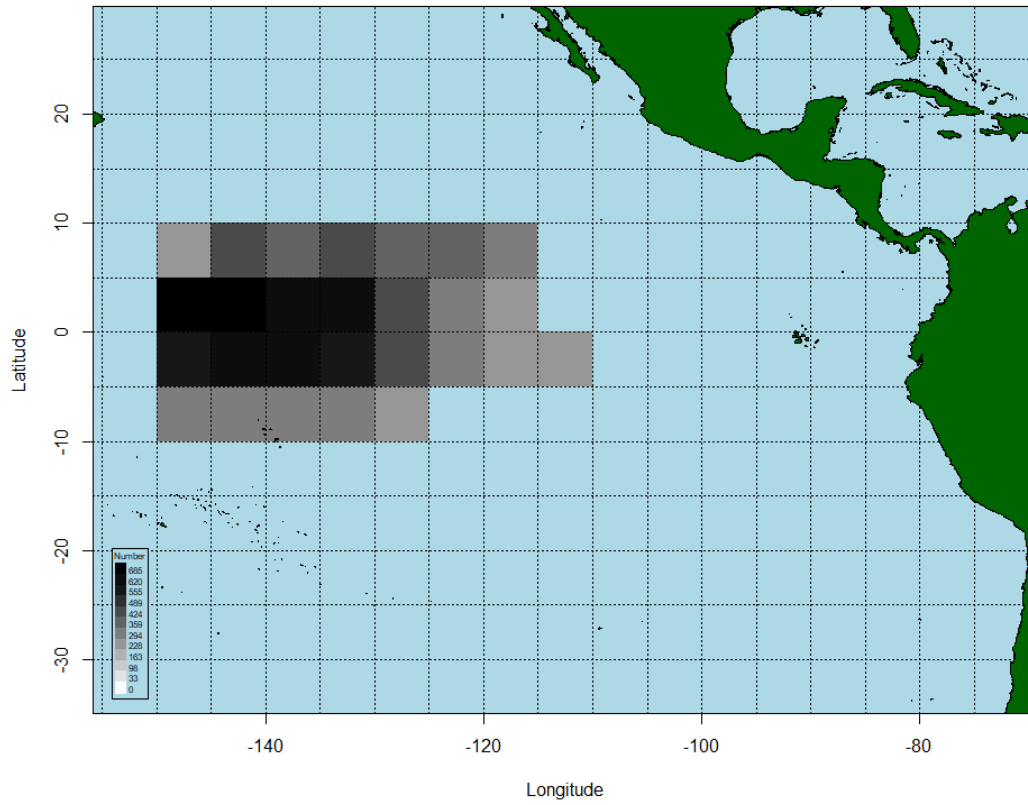


**Figure 5.** Spatial distribution [5°x5°] of the “virgin” sequences of buoy trajectories that have been used in the GLM analysis.

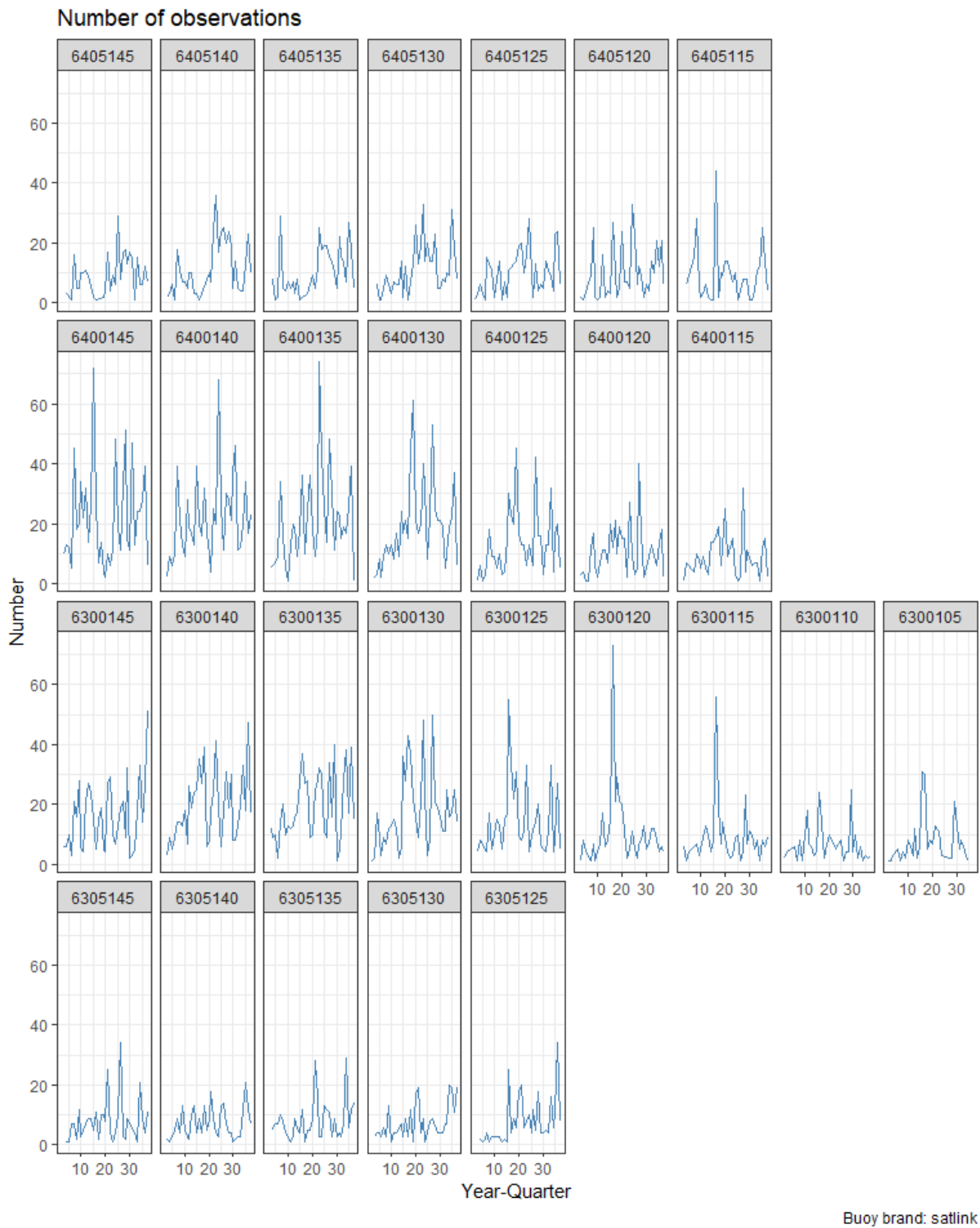


**Figure 6.** Quarterly evolution of the number of observations (“virgin” sequences of buoy trajectories) on a 5°x5° grid.



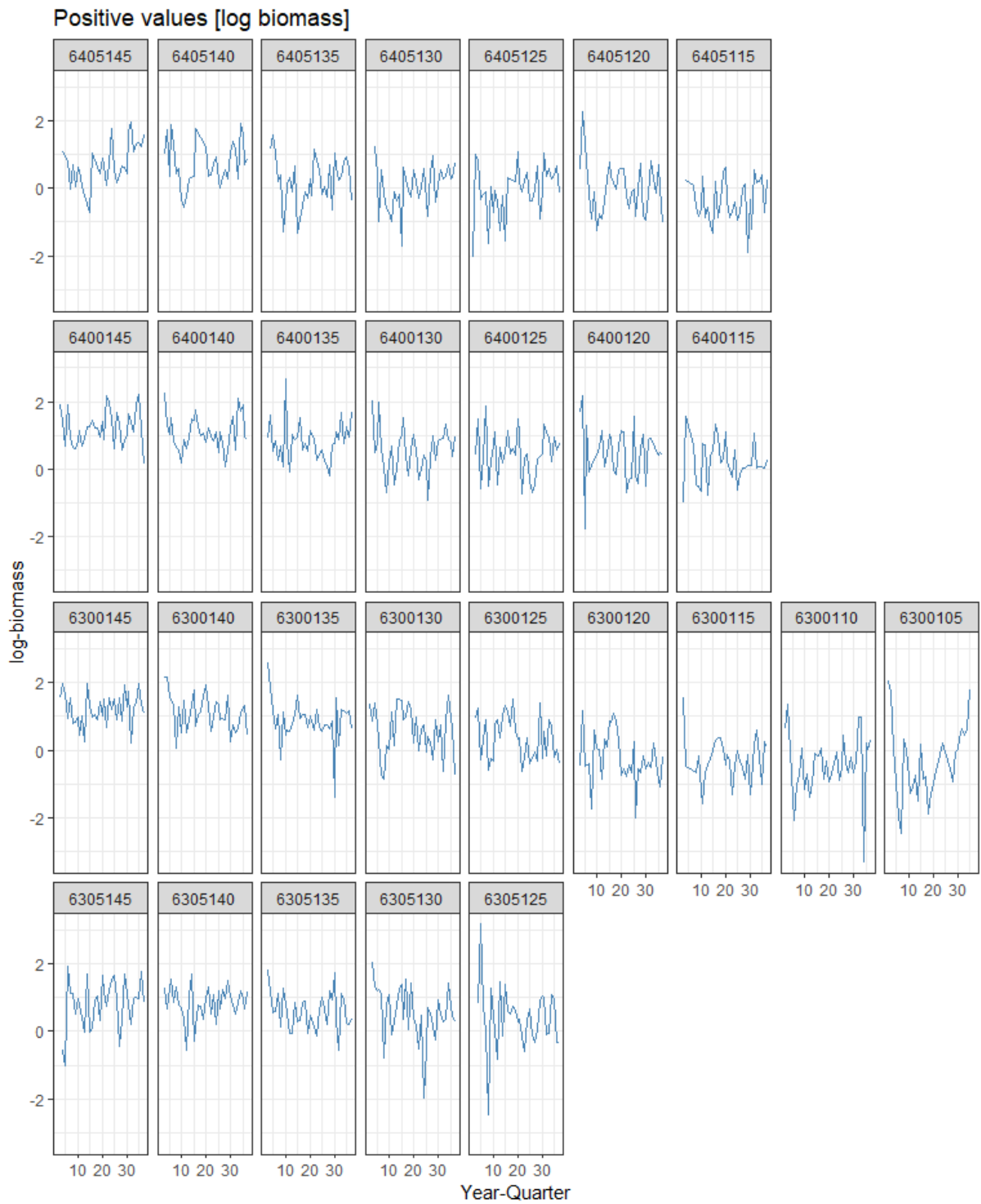


**Figure 7.** Quarterly evolution of the nominal log BAI index in the Atlantic Ocean by squares of 5x5 degrees from 2012 to 2020.

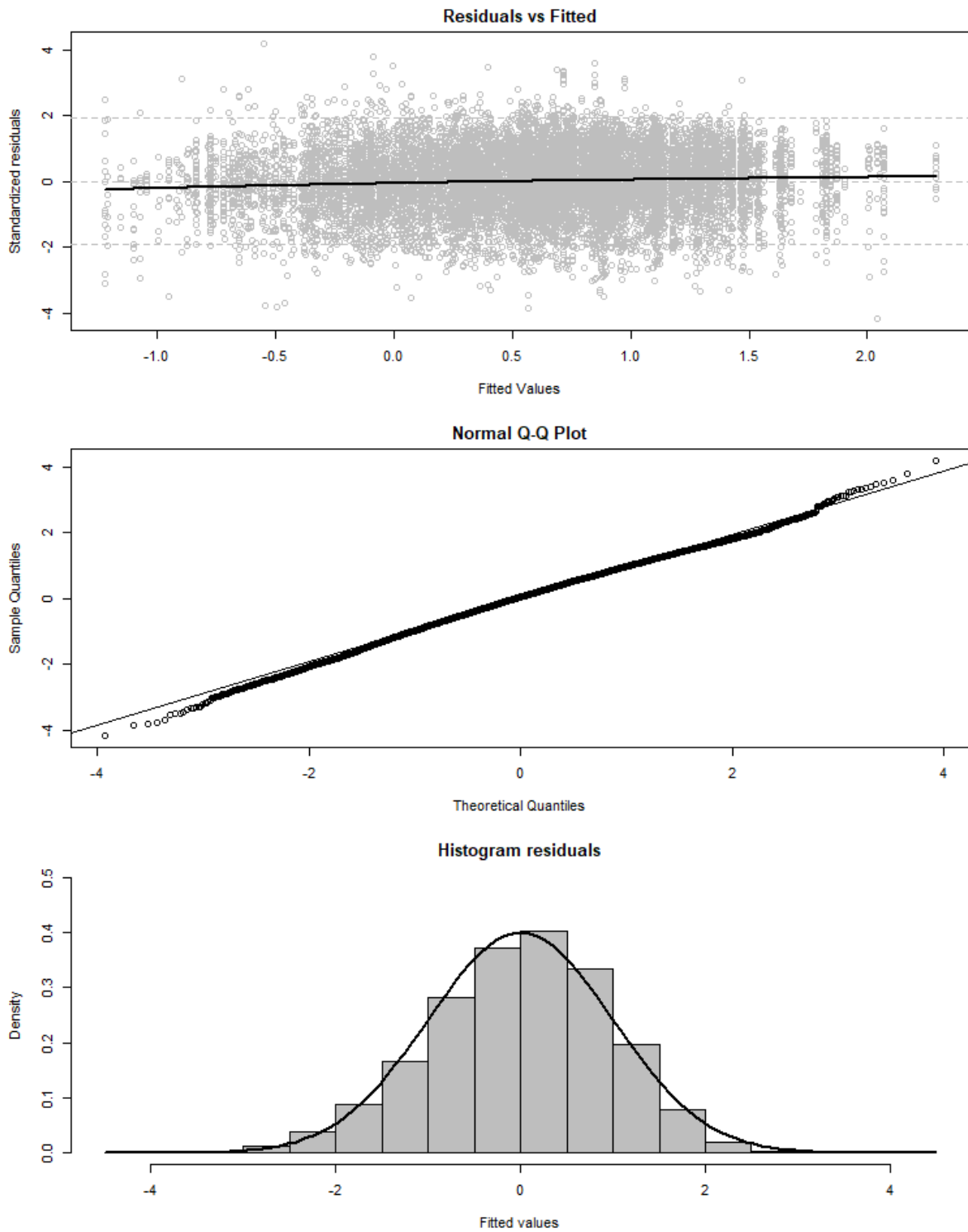


**Figure 8.** Diagnostics of the lognormal model selected for the period 2012-2020: residuals vs fitted, Normal Q-Q plot and frequency distributions of the residuals.

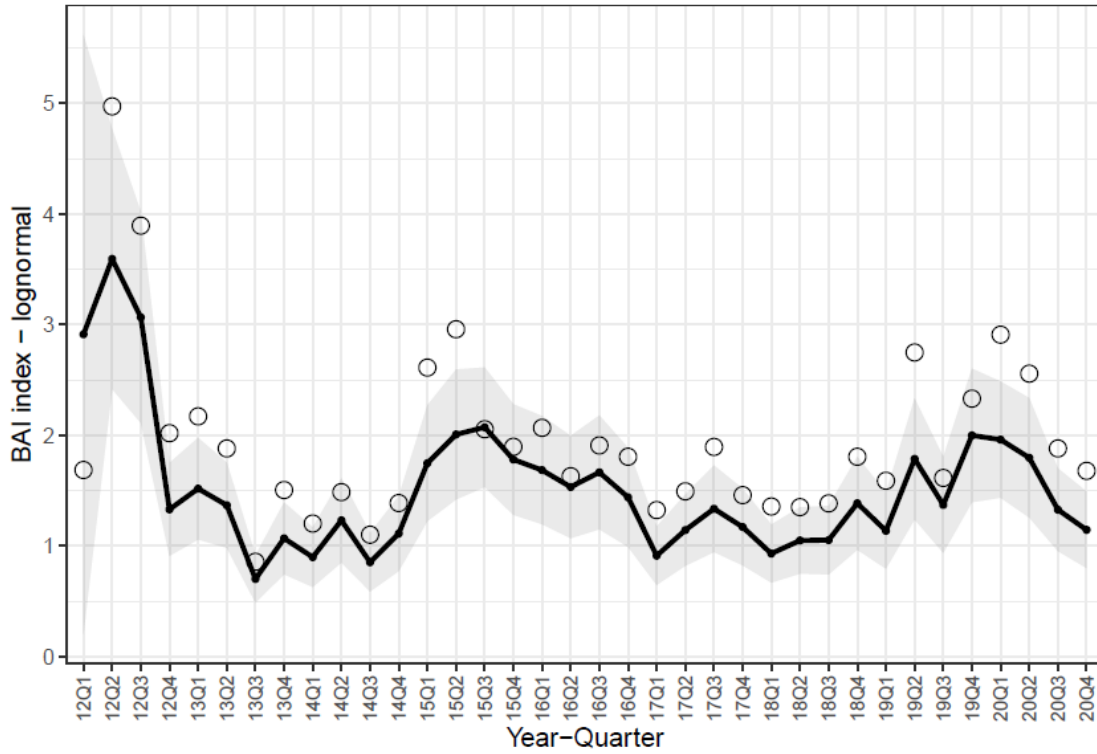


**Figure 9.** Time series of nominal (circles) and standardized (continuous line) Buoy-derived Abundance Index for the period 2012-2020. The 95% upper and lower confidence intervals of the standardized BAI index are shown by the grey shaded area.